Modelling of Temperature and Flow Fields of RF Induction Plasma (I)†

—Preliminary Calculation for Low Temperature and High Flow Rate Case—

Masao USHIO*, Fukuhisa MATSUDA** and Seishiro KAWANO***

Abstract

A preliminary mathematical formulation has been developed to represent the velocity field and the temperature field in inductively produced RF plasma at atmospheric pressure, which is weakly ionized in high rate of gas flow. The formulation utilized an engineering approach in which the plasma was regarded as a continuum of known electrical properties. The behavior was represented by using the MHD equations and the convective heat balance relationship including the concept of turbulent nature of flow.

The calculations were carried out by specifying the torch and coil geometry and the coil current, and then governing equations were solved numerically. The frequency of coil current was fixed at 13.56MHz. Ultimately the velocity profiles and the temperature profiles within the system under the various conditions. Some combinations of gas flow rate, coil current and coil position were selceted as the parametric condition of calculation.

The theoretical prediction of temperature field and flowing behavior of plasma gas are compared and discussed with experimental results.

KEY WORDS: Plasma processing, RF Plasma, Induction plasma, Mathematical modelling, Plasma chemistry, Thermal Plasma

1. Introduction

Plasma processing of materials such as plasma synthesis, chemical vapor deposition, plasma spraying and so on, has been a indispensable technology for the new era of materials processing. Thermal plasma which is characterized with high enthalpy, high density and near LTE state, is considered to be much interesting due to its high energy content, and has a variety of applications particularly in the fields of high temperature processing above mentioned.

In order to study the basic process in the plasma and to make a suitable design of the plasma reactor(torch), it is very useful to develop the mathematical model of the plasma.

The mathematical modelling of induction plasma has already been described by some authors[1,2,3,4,], Particularly Boulos and Mostaghimi et al. and Yoshida and Akashi developed and extended their model to the prediction of plasma-particle interaction and obtained many valuable results. However, in those works the radiation loss from the produced plasma and also the turbulent behavior of plasma flow are not clearly considered.

The objective of the present paper is to formulate the mathematical model describing the temperature and flow fields of the plasma which is produced by induction coil under atmospheric pressure. Particularly as the first step for developing the superior numerical model, preliminary calculation based on simple assumptions is carried out and some results are shown. For the simplicity of calculation the low power input and high flow rate conditions are chosen and some results under the various flow rates of working gas which are induced through three coaxial nozzle and the various combinations of coil positions and coil currents, are compared with experimentaly measured one.

2. Physical Situation and Formulation

In **Fig. 1** the physical situation and coordinate system are shown. Schematic illustration of torch used in the experiment is also shown in the same figure. Nozzle part of the torch consists of three coaxial tubes made of quarts. The

† Received on May 7, 1991

* Professor
** Professor
*** Graduate student (Present address : Kawasaki Heavy Industry Co., Ltd.)

Transactions of JWRI is published by Welding Research Institute of Osaka University, Ibaraki, Osaka 567, Japan

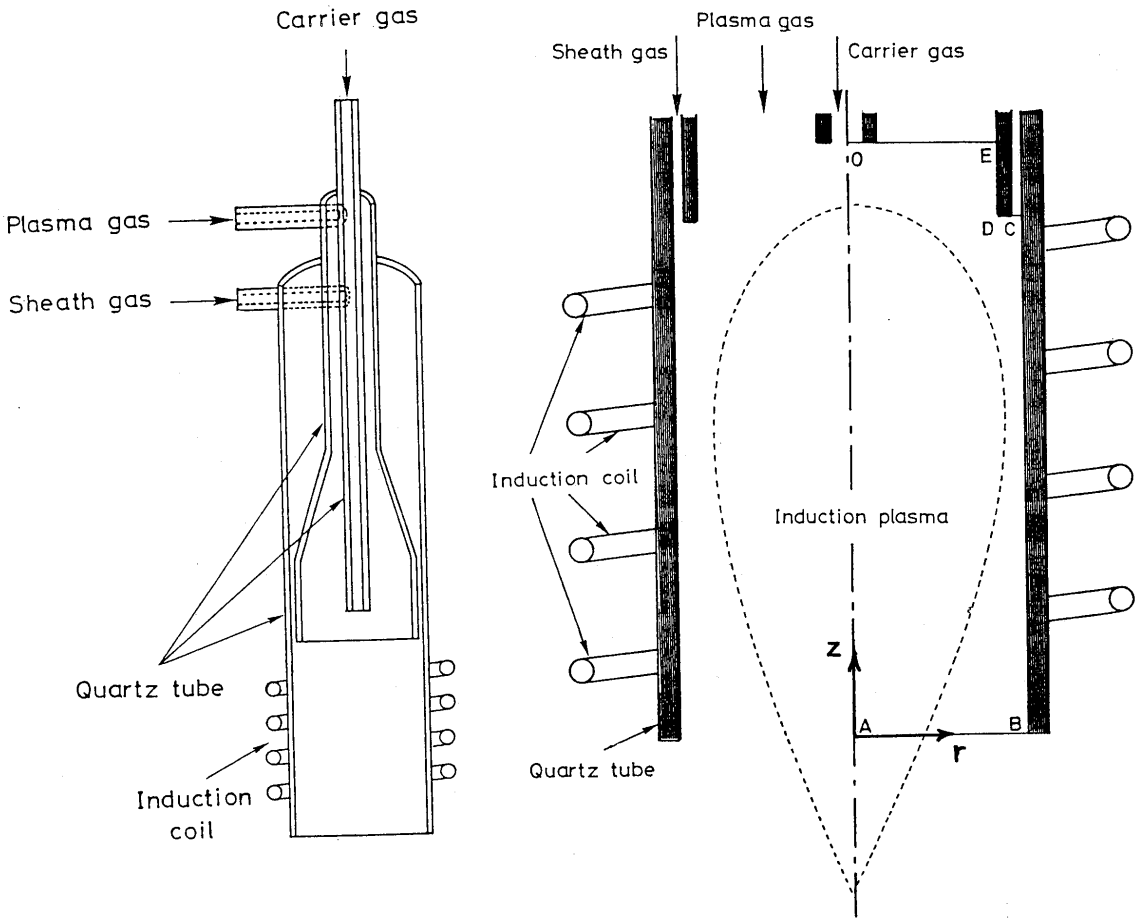

Fig. 1 Schematic illustrations of torch and inductively coupled plasma. (OA : 40 mm, BC : 35 mm, AB : 11.5 mm, OE : 10 mm)

domain to be solved is represented as OABCDEO in Fig. 1 Three different types of gas can be introduced into the torch with various flow rates respectively. Induction coil is a 4-turn coil, and a high frequency electric current (13.56 MHz) is applied to it through the auto-matching circuit. Position of the coil with respect to the torch nozzle could be adjusted freely.

The high frequency current induces a high frequency electric field and a stationally axi-symmetric plasma is produced inside the quarz tube.

The following principle assumptions are made :

1) The plasma gas is assumed to be in local thermodynamic equilibrium and optically thin.
2) The flow is steady and drived only by electromagnetic force, thus, the effect of buoyancy force is neglected. The fluid is asssumed as incompressible MHD flow.
3) The electromagnetic fields is axisymmetric, namely the magnetic field vector has z and radial components, and thus the induced electric field has only azimuthal component. The electromagnetic field is calculated in advance to the main calculation. In the case that RF power is low and the flow rate of plasma gas is high, the plasma temperature is rather low (around several thousand degree), and thus, the skin effect could be neglected.
4) Turbulent nature of plasma gas is represented in terms of K-ε model for the turbulent viscosity.
5) The transport properties of plasma gas are constant without the electrical conductivity and the values are listed in **Table 1.**

Table 1 Numerical values of parameters and constants

C_D	Dissipation constant	0.09
C_1	Constant of K-ε model	1.14
C_2	Constant of K-ε model	1.92
σ_K	Prandtl number for K	1.0
σ	Prandtl number for ε	1.3
σ_t	Turbulent Prandtl number	0.9
ρ	Mass density of Argon	0.05 kg/m^3
C_p	Specific heat	3100 J/kg K
T_B	Gas temperature at inlet	300 K
T_w	Outside wall temp. of torch	1000 K

2.1 The plasma equation

The continuity, momentum and energy equations take the following form :(Equation of continuity)

$$\nabla \cdot \boldsymbol{v}=0 \tag{1}$$

(Equation of motion)

$$\rho(\boldsymbol{v}\cdot\nabla)=-\nabla P+\mu_{eff}\nabla^2\boldsymbol{v}+\boldsymbol{F} \tag{2}$$

(Equation of energy balance)

$$\rho(\boldsymbol{v}\cdot\nabla)=\nabla\kappa_{eff}\ \nabla T+S_T \tag{3}$$

where ρ: mass density, $\boldsymbol{v}$: velocity vector, P: pressure, $\boldsymbol{F}$: body force vector (electromagnetic force vector), κ: thermal conductivity, S_T: source term which represents the Joule heat generation and radiation loss, μ: viscosity, T: temperature.

In order to determine the flow field and transport phenomena, it is necessary to solve simultaneously some additional equations which describe electromagnetic field, relationship between materials variables and turbulent properties and boudary conditions.

Upon defining the vorticity and the stream function the axisymmetric form of the equation of motion takes the following form,[5)]

Vorticity : ξ

$$\xi=\partial v_r/\partial z-\partial v_z/\partial r. \tag{4}$$

Stream function : ψ

$$v_r=-(1/\rho r)(\partial\psi r_{eff}/\delta z),\ v_z=(1/\rho r)(\delta\psi/\delta r). \tag{5}$$

Thus, the three equations are as follows:

$$\frac{\partial}{\partial z}\left(\frac{\xi}{r}\frac{\partial\psi}{\partial r}\right)-\frac{\partial}{\partial r}\left(\frac{\xi}{r}\frac{\partial\psi}{\partial z}\right)-\mu_{\text{eff}}\frac{\partial}{\partial r}\left\{\frac{1}{r}\frac{\partial}{\partial r}(r\xi)\right\}-\mu_{\text{eff}}\frac{\partial}{\partial z}\left\{\frac{1}{r}\frac{\partial}{\partial z}(r\xi)\right\}-\rho\left(\frac{\partial F_r}{\partial z}-\frac{\partial F_z}{\partial r}\right)=0 \tag{6}$$

$$\frac{\partial}{\partial z}\left(\frac{1}{\rho r}\frac{\partial\psi}{\partial z}\right)+\frac{\partial}{\partial r}\left(\frac{1}{\rho r}\frac{\partial\psi}{\partial r}\right)+\xi=0 \tag{7}$$

$$C_p\left\{\frac{\partial}{\partial z}\left(T\frac{\partial\psi}{\partial r}\right)-\frac{\partial}{\partial r}\left(T\frac{\partial\psi}{\partial z}\right)\right\}-K_{eff}\left\{\frac{\partial}{\partial r}\left(r\frac{\partial T}{\partial r}\right)+\frac{\partial^2 T}{\partial z^2}\right\}-rS_T=0 \tag{8}$$

where, μ_{eff}: the effective viscosity is defined as

$$\mu_{eff}=\mu_t+\mu_l. \tag{9}$$

And also following relationship is used

$$\kappa=C_p\ \mu_{eff}/P_r \tag{10}$$

where, P_r: Prandtl number of gas, C_p: specific heat.

The turbulent viscosity μ_t has been represented in terms of the K-ε

model

$$\mu_t=C_D\ \rho K^2/\varepsilon, \tag{11}$$

where, C_D: dissipation constant, K: turbulent kinetic energy per unit mass, ε: dissipation rate of turbulent energy. K and ε are determined by solving the following conservation equations,

$$\frac{\partial}{\partial z}\left(K\frac{\partial\psi}{\partial r}\right)-\frac{\partial}{\partial r}\left(K\frac{\partial\psi}{\partial z}\right)-\frac{\mu_{\text{eff}}}{\sigma_k}\left\{\frac{\partial}{\partial r}\left(r\frac{\partial K}{\partial r}\right)+\frac{\partial}{\partial z}\left(r\frac{\partial K}{\partial z}\right)\right\}-rS_K=0 \tag{12}$$

$$\frac{\partial}{\partial z}\left(\varepsilon\frac{\partial\psi}{\partial r}\right)-\frac{\partial}{\partial r}\left(\varepsilon\frac{\partial\psi}{\partial z}\right)-\frac{\mu_{\text{eff}}}{\sigma_\varepsilon}\left\{\frac{\partial}{\partial r}\left(r\frac{\partial\varepsilon}{\partial r}\right)+\frac{\partial}{\partial z}\left(r\frac{\partial\varepsilon}{\partial z}\right)\right\}-rS_\varepsilon=0 \tag{13}$$

The source terms S_K and S_ε are defined as

$$S_K=2\mu_t\left\{\left(\frac{\partial v_z}{\partial z}\right)^2+\left(\frac{v_r}{r}\right)^2+\left(\frac{\partial v_r}{\partial r}\right)^2+\frac{1}{2}\left(\frac{\partial v_r}{\partial z}+\frac{\partial v_z}{\partial r}\right)^2\right\}-\rho\varepsilon \tag{14}$$

$$S_\varepsilon=2C_1\mu_t\frac{\varepsilon}{K}\left\{\left(\frac{\partial v_z}{\partial z}\right)^2+\left(\frac{v_r}{r}\right)^2+\left(\frac{\partial v_r}{\partial r}\right)^2+\frac{1}{2}\left(\frac{\partial v_r}{\partial z}+\frac{\partial v_z}{\partial r}\right)^2\right\}-C_2\rho\frac{\varepsilon^2}{K} \tag{15}$$

Here, σ_K and σ_ε are the effective Prandtl number for transport of K and ε respectively. C_1, C_2 and C_D are constants and the values are listed in Table 1.

Thus, a set of equations to be solved, (6), (7), (8), (12) and (13) are obtained.

2.2 The boundary conditions

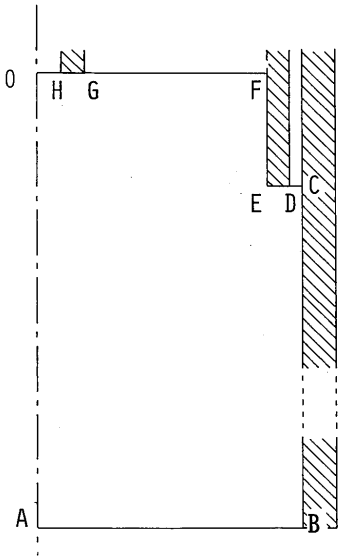

Fig. 2 Domain to be calculated in modelling.

The physical domain over which the bounadary conditions are specified are sketched in **Fig. 2** as OABCDEFGH-O. In a physical sense the bounadary conditions will specify:

1) the velocity distributions at the gas inlet,
2) the temperature distributions at the torch wall,
3) non slip conditions at the wall surface and acisymmetry about the central axis.

The velocity distributions at the gas inlets are given from pipe flow data. On CD and FG,

$$V_r=0, \tag{16}$$

$$v_z=\frac{2Q_o}{\pi\rho}\left\{r_o^2-r^2+\frac{(r_o^2-r_i^2)\log(r/r_o)}{\log(r_o/r_i)}\right\}\Big/ \left\{r_o^4-r_i^4-\frac{(r_o^2-r_i^2)^2}{\log(r_o/r_i)}\right\}, \tag{17}$$

where, Q_o : flow rate of gas, r_o : radius of C or F, r_i : radius of D or G.

Remaining boundary conditins are given as follows :

On OH,

$$v_r=0, \tag{18}$$

$$v_z=(2Q_o/\pi\rho r_o^2)\left\{1-(r/r_o^2)\right\},\ r_o=\overline{OH} \tag{19}$$

Along OA,

$$v_r=\frac{\partial v_z}{\partial r}=\frac{\partial T}{\partial r}=\frac{\partial K}{\partial r}=\frac{\partial \varepsilon}{\partial r}=0. \tag{20}$$

On AB,

$$v_r=\frac{\partial v_z}{\partial z}=\frac{\partial T}{\partial z}=\frac{\partial K}{\partial z}=\frac{\partial \varepsilon}{\partial z}=0. \tag{21}$$

On BC and EF

$$v_r=v_z=K=\varepsilon=0, \tag{22}$$

$$\frac{\partial T}{\partial r}=\frac{\kappa_w}{\kappa_f d}(T-T_w). \tag{23}$$

On DE and GH,

$$v_r=v_z=K=\varepsilon=0. \tag{24}$$

On OH, FG, and CD

$$\frac{\partial K}{\partial z}=\frac{\partial \varepsilon}{\partial z}=0. \tag{25}$$

On OHGFEDC

$$T=T_B. \tag{26}$$

2.3 Electromagnetic field

Electromagnetic field induced by the coil was obtained assuming the coil provide a complete loop current as

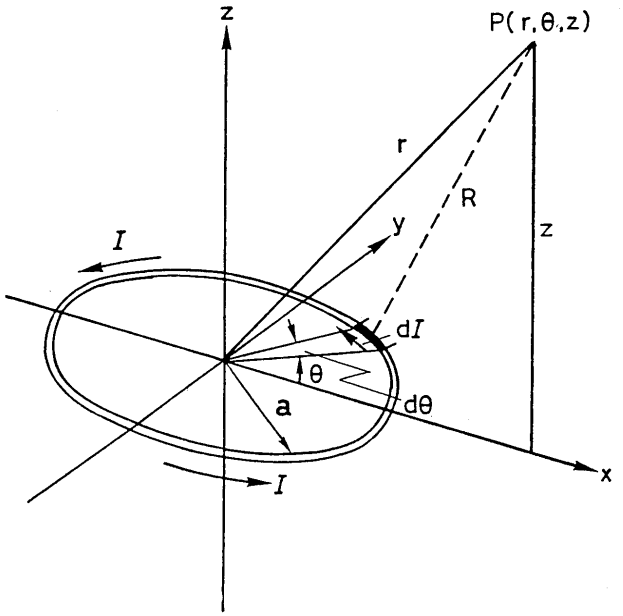

Fig. 3 Schematic view of calculation for electromagnetic field induced by a loop current.

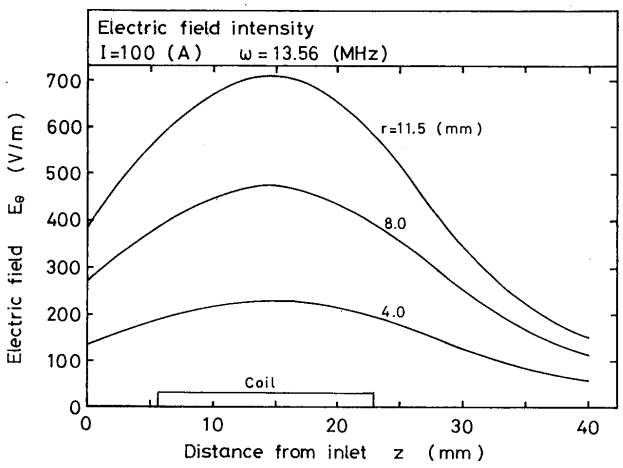

Fig. 4 An example of calculated results of time averaged electric field intesity.

shown in **Fig. 3**, which is represented as follows.

$$I = I_o \sin\omega t, \text{ (coil current)} \tag{27}$$

$$E_\theta = \frac{\mu_o I a \omega \cos\omega t}{4\pi} \int_0^{2\pi} \cdot \frac{\cos(\theta'-\theta)d\theta'}{\{(r\cos\theta - a\cos\theta')^2 + (r\sin\theta - a\sin\theta')^2 + z^2\}^{1/2}} \tag{28}$$

Thus, the time averaged values of field quantities are as follows.

$$B_r = \frac{\mu_o I a}{4\pi} \int_0^{2\pi} \frac{z\cos\theta}{\sqrt{\{(r-a\cos\theta)^2 + a^2\sin^2\theta + z^2\}^3}} d\theta, \tag{29}$$

$$B_z = \frac{\mu_o I a}{4\pi r} \int_0^{2\pi} \frac{\cos\theta}{\sqrt{\{(r-a\cos\theta)^2 + a^2\sin^2\theta + z^2\}^3}} d\theta, - \frac{\mu_o I a}{4\pi} \int_0^{2\pi} \frac{(r-a\cos\theta)\cos\theta}{\sqrt{\{(r-a\cos\theta)^2 + a^2\sin^2\theta + z^2\}^3}} d\theta, \tag{30}$$

$$E_B = \frac{\mu_o I a \omega}{4\pi} \int_0^{2\pi} \frac{\cos\theta}{\sqrt{(r-a\cos\theta)^2 + a^2\sin^2\theta + z^2}} d\theta. \tag{31}$$

Actually the coil has 4 turns, then the contributions of individual loop current was superposed. Electric field intensity calculated was shown in **Fig. 4** for the case of

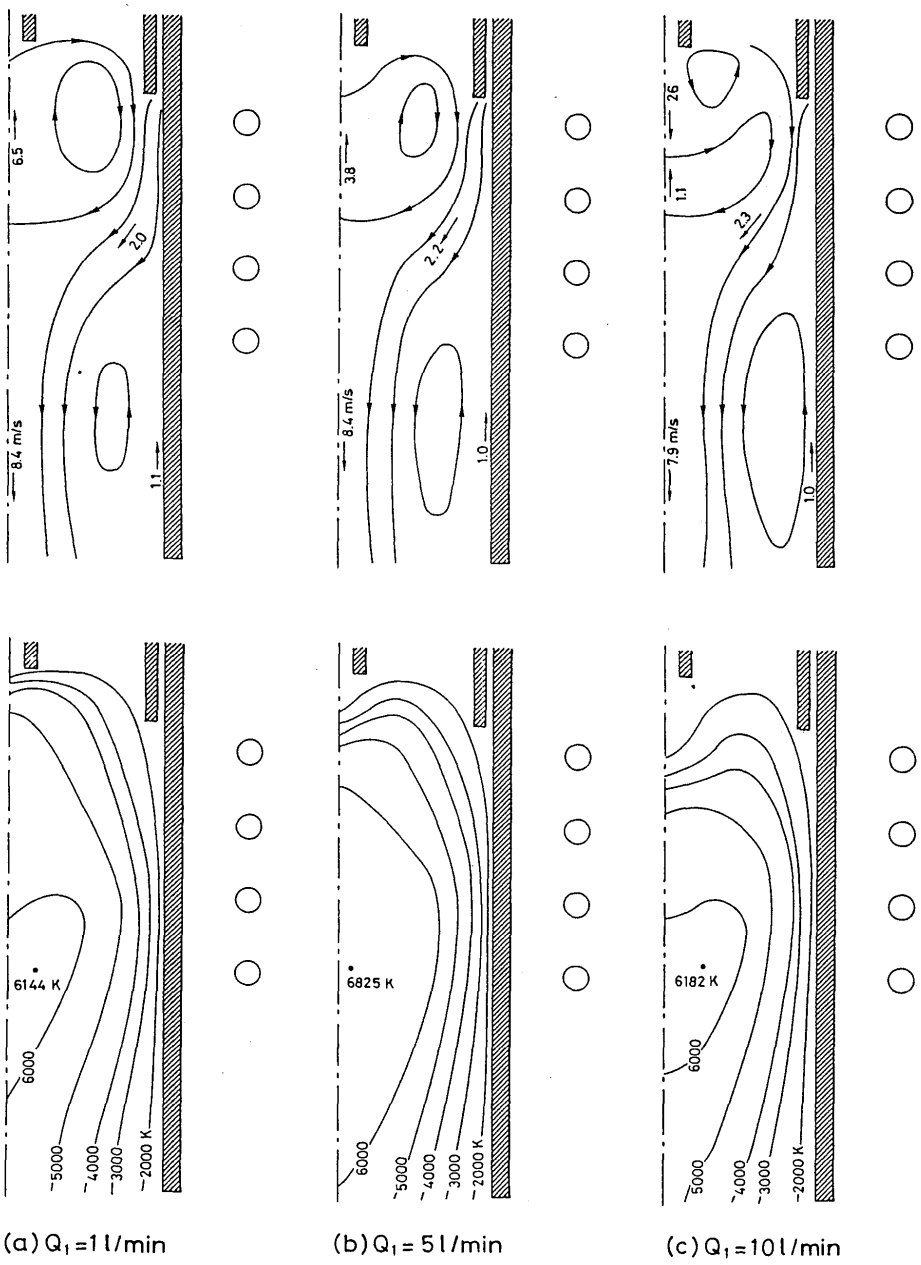

(a) Q_1 = 1 l/min (b) Q_1 = 5 l/min (c) Q_1 = 10 l/min

Fig. 5 Effect of carrier gas flow rate on flow field and temperature distribution of the plasma.

4-turns coil with 100 A in coil current and 13.56 MHz in frequency.

The volumetric rate of heat generation due to Joule heating is

$$W = \sigma \mid E \mid^2, \tag{31}$$

where, $\sigma = \sigma(T)$: electrical conductivity of gas.

Body force vector is represented as follows.

$$\boldsymbol{F} = \sigma \boldsymbol{E} \times \boldsymbol{B}. \tag{32}$$

Physical constants used in the calculation are listed in Table 1. Electrical conductivity is treated as a function of temperature.

3. Solution Procedure

The equations were put in dimensionless finite difference forms using 88×31 non-uniform mesh grids and solved numerically. Those equations were integrated over the area defined by the rectangle enclosing a grid point. Introducing the Gauss-Seidel method, point iteration process were made until the following convergence criterion could be satisfied in all variables.

$$\sum_i \sum_j \left\{ \frac{\varphi_{ij}^{(N)} - \varphi_{ij}^{(N-1)}}{\varphi_{ij}^{(N)}} \right\} \leqq \delta \tag{33}$$

where, i, j denotes the species of variables, $\varphi_{ij}^{(N-1)}$ is the

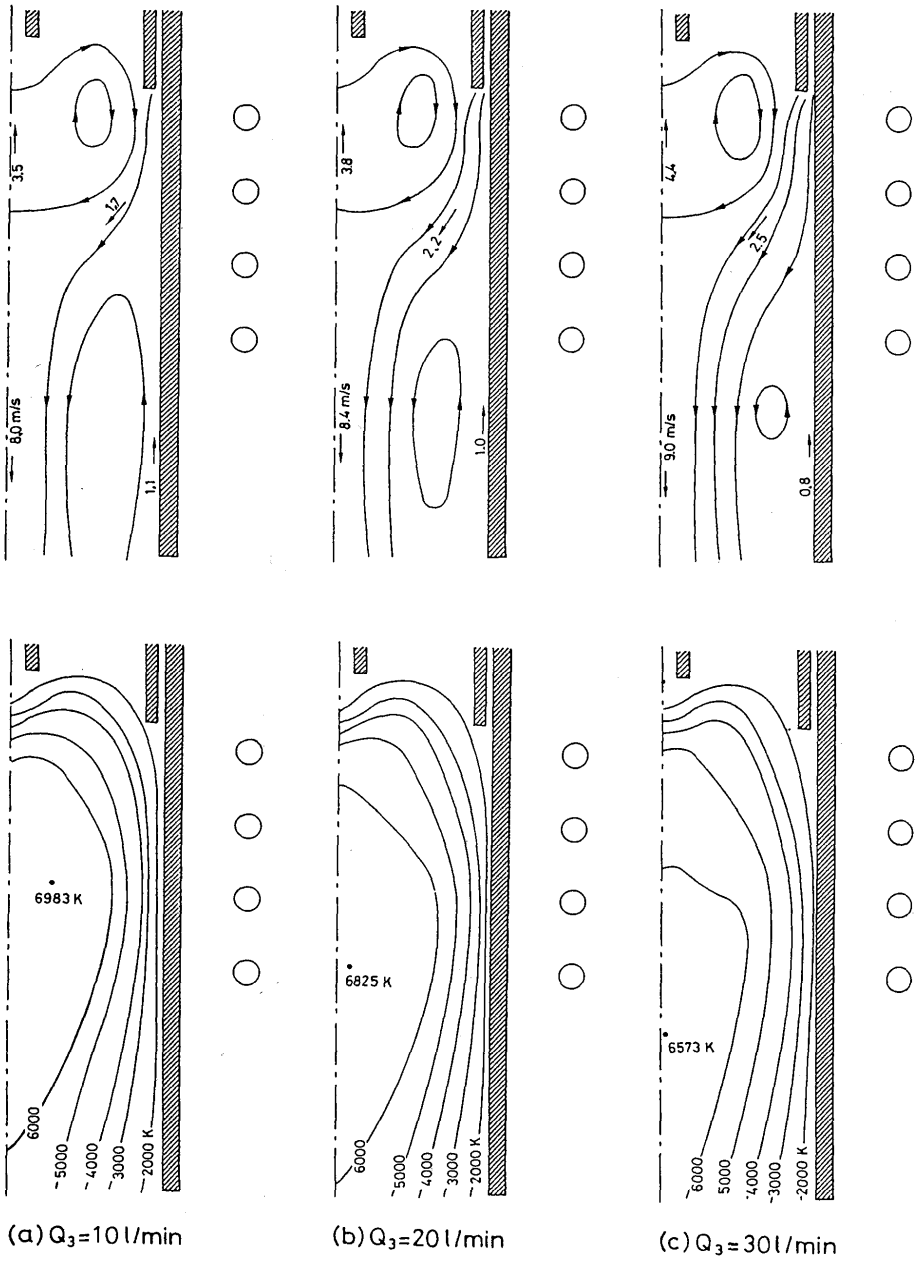

Fig. 6 Effect of sheath gas flow rate on flow field and temperature distribution of the plasma.

set to be 0.001.

4. Calculated Results and Discussions

Numerical calculations were carried out under the conditions that the coil is 4-turns and coil current is 100 A with 13.56 MHz in frequency. Gases are introduced from 3 nozzles whose flow rates are adjusted independently. From the central inlet, the carrier gas is introduced, main working gas denoted as plasma gas is introduced from the middle inlet and the cooling gas is (sheath gas) is introduced along the wall.

4.1 Effects of flow rates of central gas (carrier gas)

In **Fig. 5** effects of carrier gas flow rates on the flow field and temperature fields are shown. With increase in flow rates of carrier gas, the flow pattern of circulation flow induced in the upstream side becomes in disorder, and the temperature gradient near the gas inlet decreases.

4.2 Effects of flow rates of sheath gas and plasma gas

With increase in flow rates of sheath gas, the circulation flow in the upstream side grows and that in the downstream side decays, as shown in **Fig.6.**

In the effects of plasma gas flow rates, similar tendency is obtained.

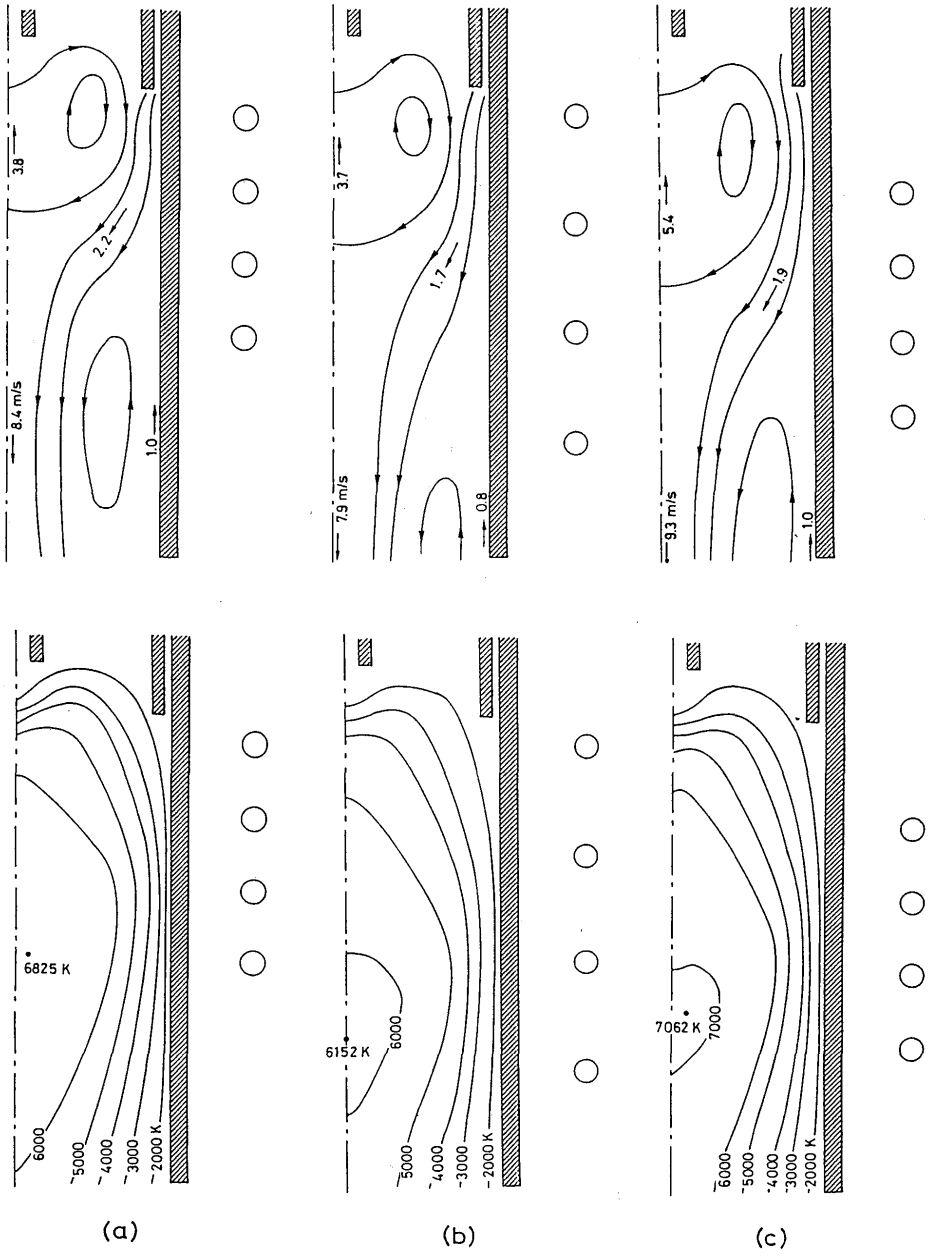

Fig. 7 Effect of coil positisn on flow field and temperature distribution of the plasma.

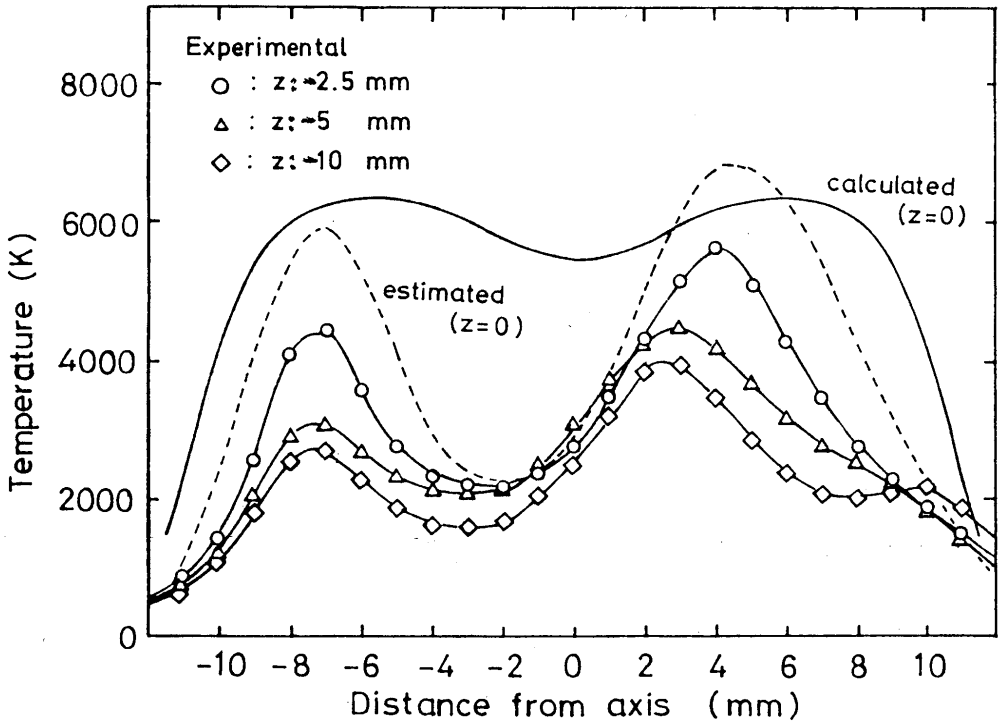

Fig. 8 Comparison between calculated and experimentally measured temperature distributions.

4.3 Effects of nozzle length of cooling gas inlet

The effect of nozzle length of cooling gas inlet, EF in **Fig. 2**, is estimated. And it is shown that within this length it has no effect on the behavior of the circulation flow in the upstream side.

4.4 Effects of coil position

Figure 7 shows the effect of coil position on the flow and temperature fields. The position of circulation flows has strong relationship with the position of coil, which could be easily expected.

And also the temperature distribution is changed by the coil space. These results suggest the design of coil is very important to generate the flow and temperature fields as required.

5. Discussions and Conclusions

The weakest point of this modelling is in the neglect of some important properties of high temperature thermal plasma, namely, the skin effect, the compressibility, temperature dependence of materials constants and so on. In **Fig. 8**, an example of comparison with experimental results, which was measured by S. Sato *et al.*, is shown.[6] The experiment was made by using similar torch but with rather high power (~3 kW). And due to optical difficlties, the measurement was carried out just at the outside of the torch. Therefore, the measured temperature distributions were extraporated to the outlet boundary of the torch and compared with calculated one. Discrepancy of the temperature distribution particularly around central axis is high.

In the case of higher coil current, plasma temperature increases and the assumption applied in the modelling increses the invalidity of calculated results. Above discrepancy is cosidered to be ascribed to these reasons.

However this modelling is considered to be useful in case of lower coil current and high flow rate, that is, in low temperature plasma. And then, some conclusions can be deduced from the calculated results as follows.

In the torch, two circulation flows appearred, and the position of the flow is closely correlated with the coil position. In order to design the RF plasma torch, the numerical modelling is indispensably useful.

References

1) J. Mostaghini, P. Proulx and M.I. Boulos; Numerical Heat transfer, Vol.8(1985), P.187–201.

2) P. Proulx, J. Mostaghini and M.I. Boulos; Int. J. Heat & Mass Transfer, Vol.28(1985), P.1327–1336.

3) E. Bourdin, P. Fauchais and M.I. Boulos; Int, J. Heat Mass Transfer, Vol.26(1983), P.567–582.

4) T. Yoshida and K. Akashi; J.Appl.Phys., Vol.48(1977), P. 2252–2260.

5) A.D. Gosman, W.M. Pun, A.K. Ruchal, D.B. Spalding and M.Wolfstein; "Heat and Mass Transfer in Recirculating Flows", Academic Press (1969).

6) S. Sato, S. Ameda, S. Uematsu, T. Senda; 1st Japan Symp. Plasma Chemistry, (1988).